

PHOTOACOUSTIC SPECTROSCOPY

by

Arzu Çolak

B.S. in Physics, İstanbul University, 2002

Submitted to the Institute for Graduate Studies in
Science and Engineering in partial fulfillment of
the requirements for the degree of
Master of Science

Graduate Program in Physics

Boğaziçi University

2006

annem ve babam için
(for my parents)

ACKNOWLEDGEMENTS

I would like to express my deepest gratitude to my thesis supervisor Prof. Dr. Yani Skarlatos for his most valuable guidance, support and encouragement throughout my study. This thesis would not be possible without his inspiring suggestions and valuable criticism.

I would like to thank Prof. Dr. Naci İnci, Prof. Dr. Ömür Akyüz, and Prof. Dr. Selim Şeker for reading my thesis and their valuable suggestions.

I also owe thanks to Assoc. Prof. Alp Osman Kodolbaş and Rıfat Kangı from the National Metrology Institute (UME) of the Scientific and Technological Research Council of Turkey (TUBITAK) for providing me the gold black thin film, Assoc. Prof. Ali Arslan Kaya and his colleagues Orhan İpek and Cem Berk from the Marmara Research Center (MAM) for helping and guiding me in the measurements of the Atomic Force Microscopy (AFM) images of gold black, Hidayet Sağlar and his colleagues from Gölcük Naval Shipyard, and UME Mechanical Atelier staffs for providing me the photoacoustic cell, Kaan Gülnihar from UME for helping to provide me a square wave generator, Dr. Cengiz Birlikseven from UME for his valuable suggestions on my thesis and my lab-mate Ali İzzet Turan for his help in setting up photoacoustic spectroscopy (PAS) system.

I would like to express my sincere gratitude to Fulya Kunter, Özlem Yılmaz, Murat Kalemci, and Yılmaz Akarsu for their continued and enthusiastic support and friendship.

I must express my gratitude to my family for their encouragement, patience, sacrifice, and understanding for the many hours of neglect during the completion of this thesis.

ABSTRACT

PHOTOACOUSTIC SPECTROSCOPY

In its broadest sense, optical spectroscopy can be defined as the study of the interaction of light with matter. Optical spectroscopy is invaluable in studies on clean media but there are several instances where it is inadequate. In order to solve this problem, several techniques were developed, but these were applicable to only a small category of materials and useful only in a small wavelength region.

In the 1970's a new optical technique was developed to study the materials that are unsuitable for the conventional transmission or reflection methodologies. This technique called photoacoustic spectroscopy or PAS, is different than the conventional technique, since the measured signals are produced only by the absorbed light absolutely converted to heat in the sample.

In this thesis, the photoacoustic spectroscopy (PAS) experimental system that was set up at the National Metrology Institute (UME) of the Scientific and Technological Research Council of Turkey (TUBITAK) in order to make spectroscopic research on solid samples is introduced. The confirmation of whether this system is working according to the Rosencwaig-Gersho (RG) theory is done. By the aid of this study, in the future, not only spectroscopic and photocalorimetric studies, but also nondestructive depth profile analysis, thickness measurement of layers and thin films will be done using the above mentioned PAS system.

ÖZET

FOTOAKUSTİK SPEKTROSKOPİ

En geniş anlamıyla, optiksel spektroskopî ışığın madde ile etkileşiminin çalışması olarak tanımlanabilmektedir. Optiksel spektroskopî açık çevreler üzerindeki çalışmalarda çok değerlidir, fakat yetersiz olduğu çeşitli örnekler de vardır. Bu problemi çözmek için, çeşitli teknikler geliştirilmiştir, ancak bunlar malzemelerin sadece küçük bir kategorisine uygulanabilmiştir ve sadece küçük bir dalgaboyu bölgesinde yararlı olmuştur.

1970'lerde, konvansiyonel geçirme ve yansıma metodolojileri için uygun olmayan malzemeleri çalışmak için yeni bir optiksel teknik geliştirilmiştir. Fotoakustik spektroskopî ya da PAS diye adlandırılan bu teknik, konvansiyonel tekniklerden farklıdır; çünkü ölçülen sinyaller, sadece malzeme içinde tamamıyla ısıya dönüşen emilmiş ışık yoluyla üretilmektedir.

Bu tezde, katı örnekler üzerinde spektroskopik araştırma yapmak için, Türkiye Bilimsel ve Teknolojik Araştırma Kurumu (TÜBİTAK)'ın Ulusal Metroloji Enstitüsü (UME)'nde kurulmuş olan PAS deney sistemi tanıtıldı. Bu sistemin Rosencwaig-Gersho (RG) teorisine uygun olarak çalışıp çalışmadığının doğrulaması yapıldı. Bu çalışma yardımıyla, gelecekte yukarıda bahsedilen PAS sistemini kullanarak, sadece spektroskopik ve fotokalorimetrik çalışmalar değil, aynı zamanda tahribatsız derinlik profili analizi, tabakaların ve ince filmlerin kalınlık ölçümleri yapılacaktır.

TABLE OF CONTENTS

ACKNOWLEDGEMENTS.....	iv
ABSTRACT.....	v
ÖZET	vi
LIST OF FIGURES	ix
LIST OF TABLES.....	xi
LIST OF SYMBOLS/ABBREVIATIONS.....	xii
1. INTRODUCTION	1
2. THE HISTORY OF PHOTOACOUSTIC SPECTROSCOPY.....	5
3. THE ROSENCWAIG - GERSHO THEORY.....	9
3.1. Optically Transparent Solids ($l_\beta > l_s$).....	13
3.1.1. Thermally Thin Solids ($\mu_s \gg l_s$; $\mu_s > l_\beta$).....	13
3.1.2. Thermally Thin Solids ($\mu_s > l_s$; $\mu_s < l_\beta$).....	13
3.1.3. Thermally Thick Solids ($\mu_s < l_s$; $\mu_s \ll l_\beta$).....	14
3.2. Optically Opaque Solids ($l_\beta \ll l_s$).....	14
3.2.1. Thermally Thin Solids ($\mu_s \gg l_s$; $\mu_s \gg l_\beta$)	14
3.2.2. Thermally Thick Solids ($\mu_s < l_s$; $\mu_s > l_\beta$).....	15
3.2.3. Thermally Thick Solids ($\mu_s \ll l_s$; $\mu_s < l_\beta$).....	15
3.3. Conclusions of Special Cases.....	16
4. PHOTOACOUSTIC SPECTROMETERS FOR SOLID SAMPLES	18
4.1. Radiation Sources.....	19
4.2. The Photoacoustic Cell	20
4.2.1. Acoustic Isolation from the Outside World	21
4.2.2. Minimization of Extraneous Photoacoustic Signal.....	21
4.2.3. Microphone Configuration.....	22
4.2.4. Means for Maximizing the Acoustic Signal	22
4.3. Data Acquisition.....	26
5. EXPERIMENTS OF PHOTOACOUSTIC SPECTROSCOPY	28
5.1. General Outline	28
5.2. General Description of Apparatus.....	29

5.3. Signal to Noise Ratio	29
5.4. The RG Theory	31
5.5. The Photoacoustic Spectrum of Carbon Black	31
5.6. The Absorption Spectrum of Blood	33
5.7. Calibration of the Photoacoustic Cell	35
6. CONCLUSIONS.....	40
REFERENCES	42

LIST OF FIGURES

Figure 2.1.	The appearance of Bell's photophone	5
Figure 3.1.	Principle of photoacoustic effect	9
Figure 3.2.	Schematic representation of the special cases for the photoacoustic theory of solids	12
Figure 4.1.	Block diagram of a typical single-beam photoacoustic spectrometer system.....	18
Figure 4.2.	A photoacoustic cell with an acoustically resonant section.....	24
Figure 4.3.	The photoacoustic cell used in experiments	25
Figure 4.4.	The photoacoustic spectrometer block diagram	27
Figure 5.1.	Signal to noise ratio of the photoacoustic system.....	30
Figure 5.2.	A log-log plot of the photoacoustic signal versus chopping frequency for lampblack.....	31
Figure 5.3.	The reference spectrum of system	32
Figure 5.4.	The spectrum of Osram XBO 450 W xenon lamp.....	33
Figure 5.5.	The absorption spectrum of blood	34
Figure 5.6.	The medium resolution AFM picture of the gold black surface.....	36
Figure 5.7.	The photoacoustic system for gold black thin film measurements.....	37

Figure 5.8. The acoustic intensity versus modulation frequency for both optical
and electrical heating of gold black..... 38

LIST OF TABLES

Table 4.1.	Thermal properties of the material.....	21
------------	---	----

LIST OF SYMBOLS/ABBREVIATIONS

a_b	Thermal expansion coefficient of backplate
a_g	Thermal expansion coefficient of gas
a_s	Thermal expansion coefficient of solid
A	Cross-sectional area of photoacoustic cell channel
c_o	Velocity of sound
d	The closest dimension between cell boundaries in a passageway
E_0	Ground state energy
E_1	Excited state energy
I_0	Incident monochromatic light flux
k_g	Thermal conductivity of gas
k_s	Thermal conductivity of solid
l_c	Length of the channel
l_g	Length of gas column
l_s	Thickness of the solid
l_β	Optical absorption length
n	An integer
P_o	Ambient pressure
Q	Amplitude of acoustic signal
T_o	Actual temperature of gas in the cell
v	Velocity of sound
V_1	Volume of nonresonant section
V_2	Volume of resonant section
α	Thermal diffusivity of the gas
β	Optical absorption coefficient of solid
γ	The ratio of specific heat
ε	Thermoviscous damping coefficient
η_e	Effective viscosity
θ_{amb}	Ambient temperature

κ_b	Thermal conduction coefficient of backplate
κ_g	Thermal conduction coefficient of gas
κ_s	Thermal conduction coefficient of solid
λ	Wavelength of incident light
μ_b	Thermal diffusion length of backplate
μ_g	Thermal diffusion length of gas
μ_s	Thermal diffusion length of solid
ρ_o	Density of the gas
ω	Chopping frequency
AFM	Atomic Force Microscopy
B&K	Brüel & Kjaer
NDT	Nondestructive Testing
PAM	Photoacoustic Microscopy
PAS	Photoacoustic Spectroscopy
PTP	Photothermophone
RG	Rosencwaig – Gersho
SNR	Signal to noise ratio
SRS	Stanford Research System
TUBITAK	The Scientific and Technological Research Council of Turkey
UME	The National Metrology Institute

1. INTRODUCTION

In its broadest sense, spectroscopy can be defined as the study of the interaction of light with matter. As such, it is a science encompassing many disciplines and many techniques. In the field of high energy physics, the radiation is sufficiently energetic to seriously perturb, and in some cases, even transform the matter with which it interacts. On the other hand, in the oldest form of spectroscopy, optical spectroscopy, the energy is usually too low to perturb or noticeably alter the material under study. Because of its versatility, range, and nondestructive nature, optical spectroscopy remains a widely used and most important tool for investigating and characterizing the properties of matter.

Conventional optical spectroscopies tend to fall in to two major categories [1]. The first category involves the study of the optical photons that are transmitted through the material of interest, that is, the study of those photons that did not interact with the material. The second category involves the study of the light that is scattered or reflected from the material, that is, those photons that have undergone some interaction with the material. Almost all conventional optical methods are variations on these two basic techniques. As such, they are distinguished not only by the fact that optical photons constitute the incident energy beam, but also by the fact that the data are obtained by detecting some of these photons after the beam has interacted with the matter or material under investigation.

Optical spectroscopy has been a scientific tool for over a century, and it has proven invaluable in studies on reasonably clean media, such as solutions and crystals, and on specularly reflective surfaces. There are, however, several instances where conventional transmission spectroscopy is inadequate even for the case of clear, transparent materials. Over the years, several techniques have been developed to permit optical investigation of highly light-scattering and opaque substances. All these techniques have proven to be very useful; yet, each suffers from serious limitations. In particular, each method is applicable to only a relatively small category of materials, each is useful only over a small wavelength range, and the data obtained are often difficult to interpret.

In the 1970s, another optical technique developed to study those materials that are unsuitable for the conventional transmission or reflection methodologies [2]. This technique, called photoacoustic spectroscopy or PAS, is different than the conventional techniques chiefly in that even though the incident energy is in the form of optical photons, the interaction of these photons with the material under investigation is studied not through subsequent detection and analysis of some of the photons, but rather through a direct measure of the energy absorbed by the material as a result of its interaction with the photon beam.

In photoacoustic spectroscopy, the sample to be studied is often placed in a closed cell or chamber. For the case of gases and liquids the sample generally fills the entire chamber. In the case of solids, the sample fills only a portion of the chamber, and the rest of the chamber is filled with a nonabsorbing gas such as air. In addition, the chamber also contains a sensitive microphone. The sample is illuminated with monochromatic light that either passes through an electromechanical chopper or is intensity modulated in some other fashion. If any of the incident photons are absorbed by the sample, internal energy levels within the sample are excited. Upon subsequent deexcitation of these energy levels, all or part of the absorbed photon energy is then transformed into heat energy through nonradiative deexcitation processes. In a gas this heat energy appears as kinetic energy of the gas molecules, while in a solid or liquid, it appears as vibrational energy of ions or atoms. Since, the incident radiation is intensity modulated, the internal heating of the sample is also modulated.

Since photoacoustics measures the internal heating of the sample, it clearly is a form of calorimetry, as well as a form of optical spectroscopy. That is to say photoacoustic is a combination of optical spectroscopy and calorimetry. Although a more appropriate name for the technique might be photocalorimetry, for this methodology whether it employs microphones or piezoelectric detectors the term photoacoustics is used.

There are several advantages to photoacoustics as a form of spectroscopy, that is, when it is used to perform photoacoustic spectroscopy, since absorption of optical or electromagnetic radiation is required before a photoacoustic signal can be generated, light that is transmitted or elastically scattered by the sample is not detected and hence does not

interfere with the inherently absorptive PAS measurements.

Another advantage is the capability of obtaining optical absorption spectra on materials that are completely opaque to transmitted light since the technique does not depend on the detection of photons. Coupled with this is the capability, unique to photoacoustic spectroscopy, of performing nondestructive depth-profile analysis of absorption as a function of depth in a material.

Furthermore, since the sample itself constitutes the electromagnetic radiation detector, no photoelectric device is necessary, and thus studies over a wide range of optical and electromagnetic wavelengths are possible without the need to change detector systems. The only limitations are that the source be sufficiently energetic and that whatever windows are used in the system be reasonably transparent to the radiation. Finally, the photoacoustic effect results from a radiationless energy conversion process and is therefore complementary to radiative and photochemical processes.

Photoacoustics is, however, much more than spectroscopy. It is, after all, a photocalorimetric method that measures how much of the electromagnetic radiation absorbed by a sample is actually converted to heat. As such, photoacoustics can be used to measure the absorption or excitation spectrum, the lifetime of excited studies, and the energy yield of radiative processes. These are all spectroscopic measurements. On the other hand photoacoustics can also be used to measure thermal and elastic properties of materials, to study chemical reactions, to measure thicknesses of layers and thin films, and to perform a variety of other nonspectroscopic investigations. In such studies, the calorimetric or acoustic aspect of photoacoustics plays the dominant role, while the photon or electromagnetic part is simply a convenient excitation mechanism.

With its various spectroscopic and nonspectroscopic attributes, photoacoustics has already found many important applications in the research and characterization of materials. Photoacoustic studies are performed on all types of materials, inorganic, organic, and biological, and on all three matter states-gas, liquid, and solid.

The aim of this thesis is to introduce the photoacoustic spectroscopy system that was set up at the National Metrology Institute (UME) of the Scientific and Technological Research Council of Turkey (TUBITAK) in order to make spectroscopic research on solid samples, and to give some examples of spectroscopic studies that were made by using this system.

The outline of the thesis is as follows. In Chapter 2, the history of photoacoustic spectroscopy will be presented. In Chapter 3, the Rosencwaig-Gersho (RG) theory, which is fundamental physical event under photoacoustic effect, will be explained. In Chapter 4, the photoacoustic spectrometers for solid samples will be introduced. In Chapter 5, the experimental part of our work will be detailed and the data obtained as a result of different measurements will be presented. Finally, in Chapter 6, a conclusion will be given.

2. THE HISTORY OF PHOTOACOUSTIC SPECTROSCOPY

Photoacoustic spectroscopy (PAS) made its first official appearance in 1973. At the beginning it referred to as optoacoustic spectroscopy, because it was a similar technique to optoacoustic spectroscopy which has been used for in the study of optical absorption phenomena in gases. But, then the name of the technique was changed from optoacoustic to photoacoustic in order to reduce confusion with the acousto-optic effect in which a laser beam is deflected by acoustic or elastic waves in a crystal [3]. However, the term of optoacoustic still uses for studies on gases in many fields, whereas the term of photoacoustic uses for the research of nongaseous material.

The photoacoustic effect in both nongaseous and gaseous matter was discovered in the nineteenth century and was first reported in 1880 by Alexander Graham Bell [4].

In short, the reason of the discovery of Bell's photoacoustic effect was his experiments with photophone which consisted of a voice-activated mirror, a selenium cell, and an electrical telephone receiver. With the voice-activated mirror the intensity of a beam of sunlight was modulated then it was focused onto the selenium cell as depicted in Figure 2.1. Because of the change of selenium's resistance with the intensity of light falling on it, the voice-modulated beam of sunlight resulted in electrically reproduced telephonic speech.

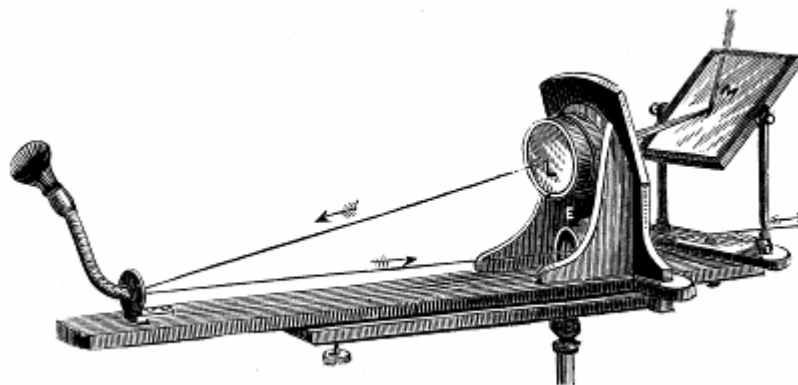


Figure 2.1. The appearance of Bell's photophone [5]

Bell discovered that it was possible to obtain, in many occasions, an audible signal directly, that is, in a non electrical fashion while he was experimenting with the photophone.

In 1881, in one of his publication, Bell stated that if solid matters which were placed inside an enclosed cell to which a hearing tube was attached, were illuminated with a periodically interrupted beam of sunlight, an audible sound could be heard. The general conclusions, arrived from a great number of experiments with solid substances, were that the loudest sounds were produced from substances in a loose, porous, spongy condition and from those that had the darkest or most absorbent colors. The materials giving the best effects were cotton wool, worsted, fibrous materials generally, cork, sponge, platinum and other metals in a spongy condition, and lampblack [5]. In short, in a series of definitive experiments, Bell showed that the photoacoustic effect in solid materials was based on the absorption of light, and for this reason, the strength of acoustical signal was based on how strongly the incident light was absorbed by the material in the cell.

Bell and his assistant also made experiments with liquids and gases. In these experiments they saw that, when the cell was filled with liquid, weak signals were produced, whereas the cell was filled with gases, more stronger signals were produced. Using the ear as a detector in these experiments was one reason of this. In spite of the fact that air was used as a coupling medium between the sample and the ear, the ear was a highly efficient way for detecting the signal with gas samples, but it was not as efficient a detector for liquid samples.

After Bell's discovery, Wilhelm Roentgen and John Tyndall, found that the photoacoustic effect could be observed for many light-absorbing gaseous substances.

As a result in the 1880s, with the contribution of fundamental gas laws which were known at that time, the photoacoustic effect was understood well for gaseous substances.

It was correctly assumed that if the gaseous substance absorbed all or part of the chopped incident light, it was itself periodically heated. This heating changed the volume and the pressure in the cell. That's to say, a pressure fluctuation occurred within the cell.

The modulation frequency of pressure fluctuation was the same as the chopping frequency. The differences of pressure were transmitted by the diaphragm of the hearing tube to its own air column and thence to the ear.

Explorers of 19th century did not experiment much, and did not attempt to explain the reason of photoacoustic signal in liquid substances. On the other hand, several attempts were made to account for the photoacoustic effect in solids, although only recently a satisfactory quantitative theory has been formulated.

In addition, Lord Rayleigh made experiments with solid samples, which were in the form of a thin flexible membrane or disk. For him, when the disk was struck by the illuminated beam of sunlight, the photoacoustical signal was detected. He concluded that the primary source for this signal was the mechanical vibration of the disk. His theory was supported by Bell. But, any optothermally induced mechanical vibrations of the solid, were too small to be the sole cause of the observed acoustic signals.

Preece, who made experiments with the photoacoustic effect, suggested that the solid did not undergo an important mechanical vibratory motion; in fact, photoacoustic effect had occurred as a result of an expansion and contraction of the air in the cell. Like Preece, Mercandier, who also experimented with the effect, concluded that the sound was due to vibratory movement determined by the alternate heating and cooling produced by the intermittent radiations, in the gaseous layer adhering to the solid surface hit by radiation [3].

After the initial flurry of interest generated by Alexander Graham Bell's original work, experimentation with the photoacoustic effect apparently ceased. The effect was seen as an interesting curiosity which didn't have any scientific or practical value. As a result of using the investigator's ear as a signal detector, the experiments were difficult to perform and quantify. So the photoacoustic effect lay dormant for nearly 50 years, until the microphone was invented. However until the beginning of 1970, the photoacoustic effect of nongaseous matter was not examined.

The first, modern quantitative theory was made in 1973 by Parker. When he performed photoacoustic experiments with gases, he measured a small photoacoustic signal emanating from cell windows. Then he derived PAS signal that could be measured as a result of weak absorptions in transparent windows. Parker found out, that his experimental results were only explained by assuming that there was abnormally big optical absorption at the surface of the cell's windows.

A few years later, Rosencwaig and Gersho formulated a good theory. This theory, now commonly referred to as the RG theory, shows that in a gas-microphone measurement of a PAS signal, the signal depends both on the generation of an acoustic pressure disturbance at substance-gas interface and on the transport of this disturbance through gas to the microphone [4]. The creation of a pressure disturbance on the surface depends on the periodic temperature at the substance-gas interface. The RG theory derives exact expressions for this temperature, while it treats the transport of the disturbance in the gas in an approximate heuristic manner, which is, however, valid for most experimental conditions.

In the following years, Bennett, Former, Aamodt, Wetsel and McDonald, by using Navier-Stokes equation and applying the transport of the acoustical disturbance in the gases more exactly, improved the theory.

As a result, near the resonant frequency of the cell and at low frequencies they were able to account for observed deviations from the RG theory. McDonald and Wetsel improved the theory a little more by adding the contribution of thermally induced vibrations in the sample.

3. THE ROSENCWAIG – GERSHO THEORY

Photoacoustic spectroscopy is different from conventional techniques chiefly in that even though the incident energy is in the form of optical photons, the interaction of these photons with the material under investigation is studied not through subsequent detection and analysis of some of the photons, but rather through a direct measure of the energy absorbed by the material as a result of its interaction with the photon beam. However, it is not necessary to apply a new universal feature of matter in order to explain the photoacoustic effect; because, as shown in Figure 3.1, the event is only conversion of light energy, which was absorbed by sample, to thermal energy.

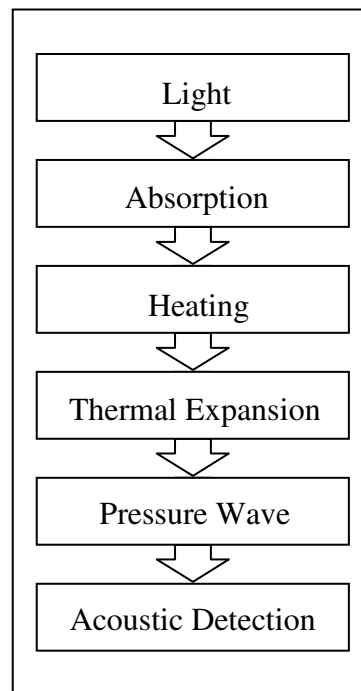


Figure 3.1. Principle of photoacoustic effect [6]

If the sample's molecule absorbs a photon, it goes from its ground state E_0 to an excited state E_1 . Then the molecule loses this energy and returns to the ground state in the following ways:

- It can reradiate a photon – radiative deexcitation.

- It can initiate a photochemical event such as bond rearrangement – photochemistry
- It can collide with another molecule of the same species that is in the ground state E_0 and excite it to its excited state E_1 – intersystem energy transfer.
- It can collide with another molecule of different species in the gas and transfer energy to translational or kinetic energy shared by both molecules – heating.

The sound wave detected by the microphone results from the fourth process. When an optically absorbing solid sample absorbs incident light, due to nonradiative deexcitation, this is converted internally to heat, and subsequently transferred to the gas in thermal contact with the sample [7]. As a result of this, the gas temperature increases. However, only $2\pi\mu_g$ thickness of gas is capable of responding thermally, to the temperature at the surface of solid sample where μ_g is the thermal diffusion length of gas. If the incident photon radiation is intensity modulated, the optical modulation results in a coherent modulation in the temperature of the gaseous sample. As it seems from gas laws, cyclical heating and cooling of the gas temperature produces a periodic pressure fluctuation with a modulation frequency equal to the optical modulation frequency. This pressure fluctuation is, of course, a sound wave and it can detect using a sensitive microphone and measure with a lock-in amplifier [8].

This physical event under photoacoustic effect of solid samples was explained and formalized in 1975-76 by Allan Rosencwaig and Allen Gersho. For this reason, this model is known as RG theory. According to this theory the amplitude of acoustic signal detected by microphone is given by [4]

$$Q = z \left[\frac{(r-1)(b+1)\exp(\sigma_s l_s) - (r+1)(b-1)\exp(-\sigma_s l_s) + 2(b-r)\exp(-\beta l_s)}{(g+1)(b+1)\exp(\sigma_s l_s) - (g-1)(b-1)\exp(-\sigma_s l_s)} \right] \quad (3.1)$$

in which

$$z = \frac{\mathcal{M}_0 P_0 \beta}{2\sqrt{2T_0}(\beta^2 - \sigma_s^2)\kappa_s a_g l_g} \quad (3.2)$$

$$r = (1-i) \frac{\beta}{2a_s} \quad (3.3)$$

$$b = \frac{\kappa_b a_b}{\kappa_s a_s} \quad (3.4)$$

$$g = \frac{\kappa_g a_g}{\kappa_s a_s} \quad (3.5)$$

$$\sigma = (1+i)a \quad (3.6)$$

$$a = (w/2\alpha)^{1/2} \quad (3.7)$$

and where κ is the thermal conduction coefficient, a is the thermal expansion coefficient, μ is the thermal diffusion length, β is the optical absorption coefficient of the solid sample for the wavelength λ , l_g is the length of the gas column in the cell, l_s is the thickness of the solid, I_0 is the incident monochromatic light flux, P_0 is the ambient pressure, T_0 is the actual temperature in the cell, and γ is the ratio of the specific heat.

However, the expression of Q given as in equation (3.1) is very complex. So, Rosencwaig and Gersho defined six special cases where the expression for Q becomes relatively simple. These cases were grouped according to the optical opaqueness of the solids as determined by the relation of the optical absorption length $l_\beta = 1/\beta$ to the thickness l_s of the solid. For each category of optical opaqueness, three cases, as shown in Figure 3.2, were considered according to the relative magnitude of the thermal diffusion length μ , as compared to the physical length l_s and the optical absorption length l_β . For all these cases Rosencwaig and Gersho made the following assumptions [3]

- At ordinary temperatures $T_0 \cong \theta_{amb}$ so that the time independent (d.c.) components of the temperature distribution need not be evaluated.
- For thermal expansion coefficient a and for thermal conduction coefficient κ ,

$\kappa_b a_b \cong \kappa_s a_s$. That is to say $b \cong 1$.

- For any gas and solid material $\kappa_g a_g \langle \kappa_b a_b$. That is to say $g \langle b$.

As a result of these assumptions Q becomes as [3]

$$Q = \frac{\beta Y}{\kappa_s a_g (\beta^2 - \sigma_s^2)} (r-1) [1 - \exp(-\beta l_s - \sigma_s l_s)] \quad (3.8)$$

where

$$Y = \frac{\mathcal{P}_0 I_0}{2\sqrt{2} T_0 l_g} \quad (3.9)$$

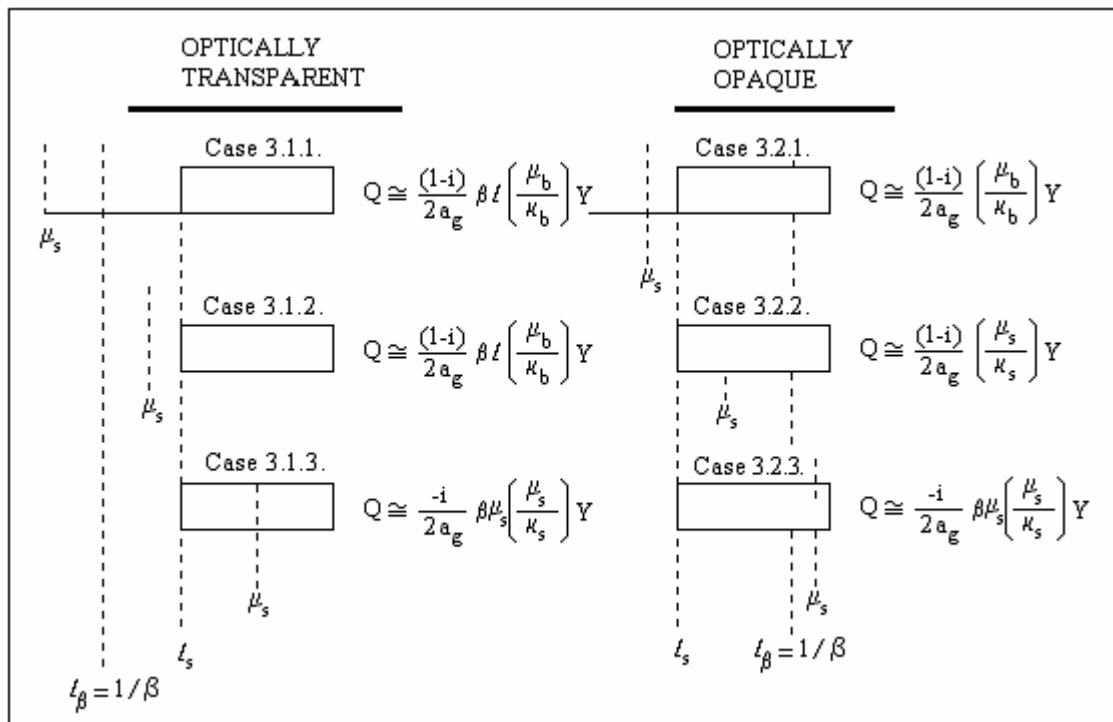


Figure 3.2. Schematic representation of the special cases for the photoacoustic theory of solids [3]

Rosencwaig and Gersho defined these special cases assuming the sample as both thermally and optically thin according to the value of l_s , μ_s and μ_b as follow [3].

3.1. Optically Transparent Solids ($l_\beta > l_s$)

For optically transparent solids, where $l_\beta > l_s$, the light is absorbed throughout the length of the samples, and some light is transmitted through the sample.

3.1.1. Thermally Thin Solids ($\mu_s \gg l_s$; $\mu_s > l_\beta$)

When $\mu_s \gg l_s$ and $\mu_s > l_\beta$, it can be assumed that $\exp(-\beta l_s) \approx 1 - \beta l_s$, $\exp(\pm \sigma_s l_s) \approx 1$ and $|r| > 1$ in equation (3.1). Then Q can be written as

$$Q = \frac{Y}{2a_g a_b \kappa_b} (\beta - 2a_s b - i\beta) \cong \frac{(1-i)\beta l_s}{2a_g} \left(\frac{\mu_b}{\kappa_b} \right) Y \propto \omega^{-1} \quad (3.10)$$

The acoustic signal is thus proportional to βl_s , and since μ_b/a_g is proportional to $1/\omega$, the acoustic signal has a ω^{-1} dependence. For this thermally thin case of $\mu_s \gg l_s$, the thermal properties of the backing material come into play in the expression for Q [3].

3.1.2. Thermally Thin Solids ($\mu_s > l_s$; $\mu_s < l_\beta$)

For thermally thin solids where $\mu_s > l_s$ and $\mu_s < l_\beta$, it is assumed that $\exp(-\beta l_s) \approx 1 - \beta l_s$, $\exp(\pm \sigma_s l_s) \approx (1 \pm \sigma_s l_s)$, and $|r| < 1$ in equation (3.1). Then Q becomes

$$Q = \frac{\beta l_s Y}{4\kappa_s a_g a_s^3 b} [(\beta^2 + 2a_s^2) + i(\beta^2 - 2a_s^2)] \cong \frac{(1-i)\beta l_s}{2a_g} \left(\frac{\mu_b}{\kappa_b} \right) Y \propto \omega^{-1} \quad (3.11)$$

The acoustic signal is again proportional to βl_s , varies as ω^{-1} , and depends on the thermal properties of the backing material. Equation (3.11) is identical to equation (3.10) [3].

3.1.3. Thermally Thick Solids ($\mu_s < l_s$; $\mu_s \ll l_\beta$)

For thermally thick solids where $\mu_s \ll l_s$ and $\mu_s \ll l_\beta$, Rosencwaig and Gersho set $\exp(-\beta l_s) \approx 1 - \beta l_s$, $\exp(-\sigma_s l_s) \approx 0$ $|r| \ll 1$ in equation (3.1). The acoustic signal then becomes

$$Q \cong -i \frac{\beta \mu_s}{2a_g} \left(\frac{\mu_s}{\kappa_s} \right) Y \propto \omega^{-3/2} \quad (3.12)$$

Here the signal is proportional to $\beta \mu_s$ rather than βl_s . That is, only the light absorbed within the first thermal diffusion length contributes to the signal, in spite of the fact that light is being absorbed throughout the length l_s of the solid. Also, since $\mu_s < l_s$, the thermal properties of the backing material presented in equation (3.11) are replaced by those of the sample. The frequency dependence of Q in equation (3.12) varies as $\omega^{-3/2}$ [3].

3.2. Optically Opaque Solids ($l_\beta \ll l_s$)

For optically opaque solids condition, where $l_\beta \ll l_s$, most of the light is absorbed within a distance that is small compared to l_s , and essentially no light is transmitted.

3.2.1. Thermally Thin Solids ($\mu_s \gg l_s$; $\mu_s \gg l_\beta$)

For thermally thin solids where $\mu_s \gg l_s$ and $\mu_s \gg l_\beta$, in equation (3.1) it can be assumed $\exp(-\beta l_s) \approx 0$, $\exp(\pm \sigma_s l_s) \approx 1$ and $|r| \gg 1$. Then Q can be defined as

$$Q \cong \frac{(1-i) \mu_b}{2a_g \kappa_b} Y \propto \omega^{-1} \quad (3.13)$$

According to RG theory, for this condition of sample, there is a photoacoustic “opaqueness” as well as optical opaqueness, in the sense that acoustic signal is independent

of β . This would be the case for a very black absorber such as carbon black. The signal is quite strong (it is $1/\beta l_s$ times as strong as that in Section 3.1.1, depends on the thermal properties of the backing material, and varies as ω^{-1} [3].

3.2.2. Thermally Thick Solids ($\mu_s < l_s$; $\mu_s > l_\beta$)

For thermally thick solids with $\mu_s \ll l_s$ and $\mu_s \gg l_\beta$ in equation (3.2) it can be assumed that $\exp(-\beta l_s) \approx 0$, $\exp(-\sigma_s l_s) \approx 0$ and $|r| > 1$. Q becomes

$$Q = \frac{Y}{2a_g a_s \kappa_s \beta} [(\beta - 2a_s - i\beta) \cong \frac{(1-i)}{2a_g} \left(\frac{\mu_s}{\kappa_s} \right) Y \propto \omega^{-1} \quad (3.14)$$

Equation (3.14) is analogous to equation (3.13), but the thermal parameters of the backing are now replaced by those of the solid. Again the acoustic signal is independent of β and varies as ω^{-1} [3].

3.2.3. Thermally Thick Solids ($\mu_s \ll l_s$; $\mu_s < l_\beta$)

For thermally thick solids where $\mu_s \ll l_s$ and $\mu_s \ll l_\beta$ it can be assumed that $\exp(-\beta l_s) \approx 0$, $\exp(-\sigma_s l_s) \approx 0$ and $|r| < 1$ in equation (3.1). Q can be written as

$$Q = \frac{-i\beta Y}{4a_g a_s^3 \kappa_s} [(2a_s - \beta + i\beta) \cong \frac{-i\beta \mu_s}{2a_g} \left(\frac{\mu_s}{\kappa_s} \right) Y \propto \omega^{-3/2} \quad (3.15)$$

This is a very interesting and important case. Optically, the solid is opaque ($\beta l_s \gg 1$). However, as long as $\beta \mu_s < 1$ (i.e., $\mu_s < l_\beta$), this solid is not photoacoustically opaque, since, as for optically transparent thermally thick solids, only the light absorbed within the first thermal diffusion length, μ_s , contributes to the acoustic signal. Thus even though this solid is optically opaque, the photoacoustic signal is proportional to β . As for optically transparent thermally thick solids, the signal is also

dependent on the thermal properties of the sample and varies as $\omega^{-3/2}$. Experimentally this case is valid for very high frequencies [3].

3.3. Conclusions of Special Cases

Sections 3.1.1, 3.1.2, and 3.1.3 for the so-called optically transparent sample demonstrate a unique capability of photoacoustic spectroscopy, to wit, the capability of obtaining a depth profile of optical absorption within a sample; that is, by starting at a high chopping frequency, optical absorption information from only a layer of material near the surface of the solid can be obtained. For materials with low thermal diffusivity this layer can be as small as 0.1 μm at chopping frequencies of 10.000-100.000 Hz. Then by decreasing the chopping frequency, the thermal diffusion length is increased and optical absorption data further within the material can be obtained, until at ~ 5 Hz data down to 10-100 μm for materials with low thermal diffusivities and up to 1-10 mm for materials with high thermal diffusivities can be obtained. This capability for depth-profile analysis is unique and opens up exciting possibilities in studying layered and amorphous materials and in determining overlay and thin film thicknesses.

The photoacoustic signal is ultimately governed by the magnitude of the thermal diffusion length, μ_s , can be changed by changing the chopping frequency, ω , a solid that is completely opaque optically need not be photoacoustically opaque. It is therefore possible with the photoacoustic technique to obtain optical absorption spectra of any but the most highly opaque solids. This capability of PAS, together with its insensitivity to scattered light, makes its use as a spectroscopic tool for the investigation of solid and semisolid materials highly attractive. These features give the photoacoustic technique a unique potential for noninvasive in vivo studies of human tissues a potential which may have important implications in biological and medical research and in medical diagnostics [9].

For thin films, the photoacoustic effect gives us a chance to see the interference of multiple reflections in the sample, and this a way of to find features of the sample.

For the region with low absorption, the photoacoustic signal is almost proportional to the optical absorption coefficient β which is high in regions where absorption is high; thus, optical absorption length μ_b is small. So, l_s and μ_s are bigger than μ_b , and as a result the photoacoustic signal saturates.

Saturation of the amplitude of photoacoustic signal Q , at regions with high absorption, is a good way to eliminate the dependence of signal on any other factors. That is to say, in order to eliminate the dependence of photoacoustic signal on both gas and backing materials optical and thermal features, the most suitable way is normalizing its intensity.

4. PHOTOACOUSTIC SPECTROMETERS FOR SOLID SAMPLES

As with other forms of spectroscopy, a photoacoustic spectrometer, in its elementary form, is composed of three main parts: a chopped variable wavelength light source, an experimental chamber or cell, and the data acquisition system as shown in Figure 4.1 [10]. All of these characteristics of the photoacoustic spectrometer system are familiar to optical spectroscopists with the exception of the cell and sample which determine the signal waveform. This waveform is found to depend in general on both the optical and thermal constants of a sample. This is in contrast to conventional spectroscopy, where the optical constants alone affect the signal [8].

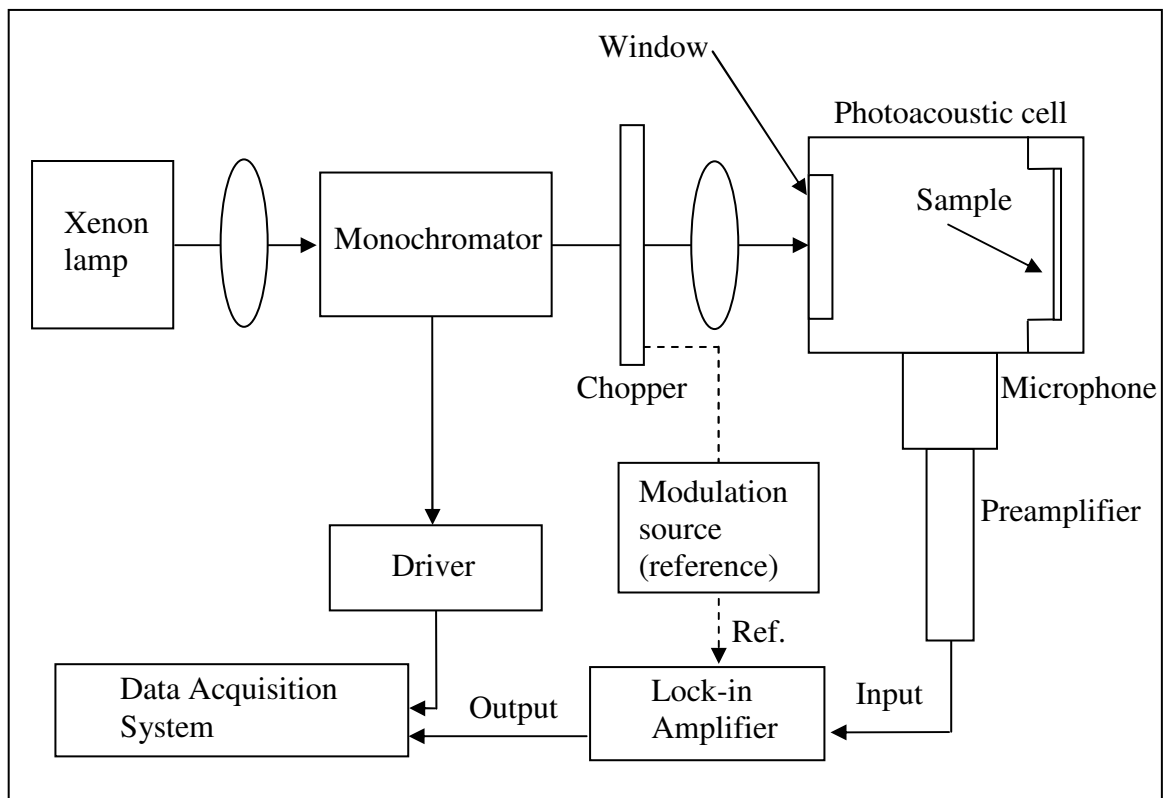


Figure 4.1. Block diagram of a typical single-beam photoacoustic spectrometer system[10]

In order to understand this spectroscopy method, the main parts of photoacoustic spectrometer should be studied step by step as explained below:

4.1. Radiation Sources

The most common and most economical sources of optical radiation in the ultraviolet, visible, and infrared regions are provided by conventional light generators. These are the arc lamp for the uv-visible, the incandescent lamp for the visible and near infrared, and the glow bar for the mid-to-far infrared regions. Since all three light sources provide a broadband optical radiation, they must be used in conjunction with suitable monochromators. The signal to noise ratio (SNR) in photoacoustic spectroscopy increases linearly with the light intensity impinging on the sample [3]. Thus, it is advantageous to use an intense light source and a high light throughput monochromator.

Under the light of this information, in our experimental system, in order to study in visible region of spectrum, an Osram XBO 450 W Ozone Free Xenon lamp was used as light source. This lamp is ideal as a tunable monochromatic source between 200 nm and 1000 nm when coupled with a single or double monochromator and radiates from 260 nm to 2400 nm [11]. As a monochromator a Jobin Yvon, Triax 550 model monochromator was used in the experiments. It is a classical Czerny-Turney monochromator in its optical configuration and has a resolution of 0.025 nm with 10 micron slits and grating with 1200 grooves/mm [12].

Since the conventional light sources generally operate in a continuous mode, a light chopper, usually electromechanical in nature, must be used. This chopper can be located before or after the monochromator. In the theory of the photoacoustic effect in solids, optical absorption spectra on completely opaque samples can be obtained, and the absorption versus depth studies can be performed, provided one is able to adjust the chopping frequency. Thus, for optimum versatility, a variable speed chopper is to be recommended.

As a result, in our experimental system the dispersed radiation from the exit slits of the Triax 550 monochromator was chopped by a Stanford Research System (SRS) 540 model variable frequency chopper which is useful for all optical chopping requirements from simple measurements to dual-beam and intermodulation experiments [13].

Another source of optical radiation which can be used in photoacoustic spectroscopy of solids is the laser. A laser requires no monochromator and if operated in a pulsed mode would also require no chopper. In visible wavelength region, dye lasers provide an intense highly monochromatic light readily tunable over a fairly large wavelength range. Dye lasers can also be used with reasonable intensity in the ultraviolet region with the aid of frequency-doubling crystals. In the infrared a discrete infrared laser [e.g., the CO and CO₂ lasers) or a tunable spin-flip Raman laser can be used to great advantage to provide intense, highly monochromatic radiation [4].

In some experiments that we made with our system, a Melles-Griot He-Ne Linearly Polarized Red Laser was used instead of xenon lamp and monochromator system. This laser gives a radiation at 633 nm in 5 mW power range with 10 mm diameter, and 1 cm⁻¹ spectral linewidth [14].

4.2. The Photoacoustic Cell

The experimental chamber or cell for a photoacoustic spectrometer for solid samples is the section containing the sample, microphone with its preamplifier and all the required optics. The actual design of this chamber varies depending on whether one is using a single-beam system employing only one photoacoustic cell, or a double-beam system containing two cells, with appropriate beam splitting optics. The photoacoustic cell generally incorporates a suitable microphone with its preamplifier. Both a conventional condenser microphone with external biasing, and an electret microphone with internal self-biasing provided from a charged electret foil, is good microphone to use.

In order to design a suitable photoacoustic cell,

- Acoustic isolation from the outside world
- Minimization of extraneous photoacoustic signals arising from the interaction of the light beam with the walls, windows and the microphone in the cell
- Microphone configuration
- Means for maximizing the acoustic signal within the cell

should be considered. For that reason, it is convenient to study these criteria in more detail as below.

4.2.1. Acoustic Isolation from the Outside World

If lock-in detection methods for analyzing the microphone signal are used, acoustic isolation is not a serious problem. However, chopping frequencies different from those present in the acoustic and vibrational spectrum of the environment should be used. In addition, the cell should be designed with good acoustic seals and with walls of sufficient thickness to form a good acoustic barrier. Some reasonable precautions to isolate the photoacoustic cell from room vibrations should also be taken.

4.2.2. Minimization of Extraneous Photoacoustic Signal

To minimize any photoacoustic signal that may arise from the interaction of the light beam with the walls and windows of the cell, windows should be as optically transparent as possible for the wavelength region of interest, and the body of the cell should be constructed out of polished aluminum or stainless steel, and plexiglas. In the first two cases, optical entry to the cell is made through a small quartz window. In the plexiglas cell, the material itself is used as window [15]. Thermal properties of these materials can be given as below:

Table 4.1. Thermal properties of the material [15]

Material	α (cm ² /sec)	κ (mW/cm ² K]	α_k
Plexiglas	0.00113	1.6	44.6
Stainless steel	0.035	150	80.2
Aluminum	0.97	2000	2031

Although the aluminum or stainless steel walls absorb some of the incident and scattered radiation, the resultant photoacoustic signal would be quite weak, as long as the thermal mass of these walls is large. A large thermal mass results in a small temperature rise at the surface, and thus a small photoacoustic signal. In addition, all inside surfaces should be kept clean to minimize photoacoustic signals from surface contaminants. The

cell should also be designed so as to minimize the amount of scattered light that can reach the microphone diaphragm.

4.2.3. Microphone Configuration

Microphones are displacement-sensitive devices, and they are sensitive to the temperature induced pressure-volume changes in a photoacoustic cell. Both cylindrical microphone and flat microphones can be used for photoacoustic research. Cylindrical microphones have the advantage of being easy to construct and have a large surface area, thereby increasing their sensitivity. A disadvantage is that they do not usually possess a flat frequency response over a large acoustic range. This can be troublesome if it is planned to do experiments at different chopping frequencies. Flat microphones are commercially available, are quite sensitive when of reasonable size and good quality, and flat microphones possess a flat frequency response over a wide acoustic range.

4.2.4. Means for Maximizing the Acoustic Signal

Since the signal in a photoacoustic cell used for solid samples varies inversely with the gas volume, the volume should be minimized [10]. However, it is important to take care not to minimize this volume to the point that the acoustic signal produced at the sample suffers appreciable dissipation to the cell window and wall before reaching the microphone.

The distance between the sample and the cell window should always be greater than the thermal diffusion length of the gas, since this boundary layer of gas acts as an acoustic piston generating the signal in the cell [3].

In longer cells, where only the acoustic wave is detected during the observation time, acoustic response is proportional to input power, and inversely proportional to cell length. In contrast, in shorter cells where acoustic and thermal waves are detected during the observation time, the peak response is not proportional to input energy and the PAS response decreases with decreasing cell length [16].

In the design of a suitable photoacoustic cell, thermo-viscous damping must be taken in to account as well, since this could be a source of significant signal dissipation on the cell boundaries. Thermo-viscous damping results in an $e^{-\varepsilon x}$ damping, where ε is a damping coefficient given by

$$\varepsilon = (1/dv)(\eta_e \omega / 2\rho_0)^{1/2} \quad (4.1)$$

where d is the closest dimension between cell boundaries in a passageway, v is the sound velocity, ω is the frequency, ρ_0 is the density of gas, and η_e is an effective viscosity which depends on both the ordinary viscosity and the thermal conductivity of the gas [17]. It should be noted, however, that whereas the thermal diffusion length varies as $1/\omega$, the thermal-viscous damping coefficient varies as $\omega^{1/2}$. Thus, while the thermal diffusion length is the predominant parameter at low frequencies, the thermo-viscous term is predominant at high frequencies. A cell that is designed to be used over a wide range of frequencies should have a minimum distance between the sample and window, and minimum passageway dimensions, of 1-2 mm.

The acoustic signal in the photoacoustic cell can be enhanced by a number of means. For example, if it is possible to operate at only one frequency, the advantage of the nonflat frequency response of a cylindrical microphone can be used. Another means is to make use of an acoustically resonant cell section with a length equal to $n\lambda/2$, where n is an integer, and λ is the acoustical wavelength. In order to achieve such a resonance effect without making the cell gas volume too large, a cell can be constructed similar to that shown in Figure 4.2. For this kind of cell resonance frequency is given by

$$\omega = c_0 \left(\frac{A}{l_c V_r} \right)^{1/2} \quad (4.2)$$

where

$$V_r = \frac{V_1 V_2}{(V_1 + V_2)} \quad (4.3)$$

and A is the cross-sectional area, and l_c is the length of the channel [15]. In this cell the sample is placed in a nonresonant section of the cell, with a resonant section of reasonably small cross-sectional area joining the sample section with the microphone. However, the use of resonant cell designs, limits one to a fixed chopping frequency.

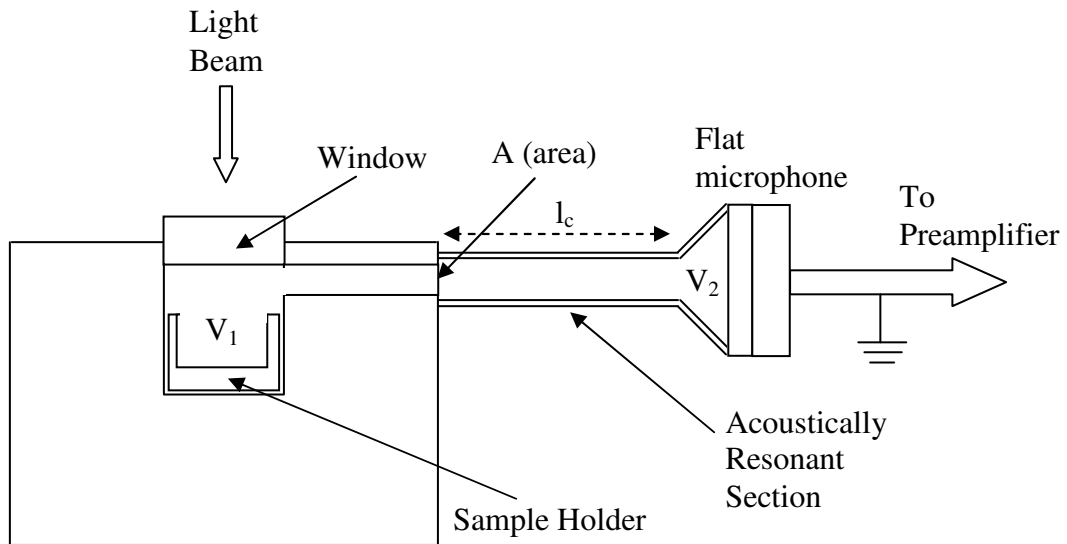


Figure 4.2. A photoacoustic cell with an acoustically resonant section [2]

Other methods to enhance the acoustic signal include the use of gases with a higher thermal conductivity, the use of higher gas pressure, and of lower gas temperatures. The theory shows that the photoacoustic signal varies in most cases as $(k_g)^{1/2}(P_0)^{1/2}/T_0$, where k_g is the gas thermal conductivity, P_0 is the pressure, and T_0 is the temperature of the gas. All these methods increase the photoacoustic signal without limiting the choice of chopping frequencies.

Consequently, with the help of all these criteria mentioned above, for our fundamental PAS system, the cell shown in Figure 4.3 was produced. The body of this cell was constructed out of a polished cylindrical block of aluminum with a large thermal mass in order to cause small temperature rise at surface. This sufficient thickness of the wall also causes a good acoustic barrier from the environment. As shown in Figure 4.3 the optical entry of the cell was made through a small quartz window in order to have an optically transparent entry for visible region. As mentioned before, the inner volume of the cell should be minimized, since the signal varies inversely with the gas volume, but it is

important to take care not to minimize this volume to the point that the acoustic signal suffers appreciable dissipation to the cell window and wall before reaching the microphone. So with paying attention to this criterion, we designed the inner cavity of cell with dimensions as shown in Figure 4.3. In the cell as the coupling gas, air at atmospheric pressure was used with α is equal to $21 \cdot 10^{-6} \text{ m}^2/\text{s}$ [18]. With the inner cavity's dimensions as drawn in Figure 4.3, and with the α parameter of air, we succeeded to construct the idea that the distance between the sample and cell window should always be greater than the thermal diffusion length of gas. In order to block the air transfer from outside to inside (or vice-versa), quartz window and microphone were sealed with o-ring. Our aim was to make experiments with changing frequency value of chopper. For that reason, we made sure to have nonresonant cell conditions. As a result we produced our cell with a high Helmholtz Resonance Frequency value according to equation (4.2).

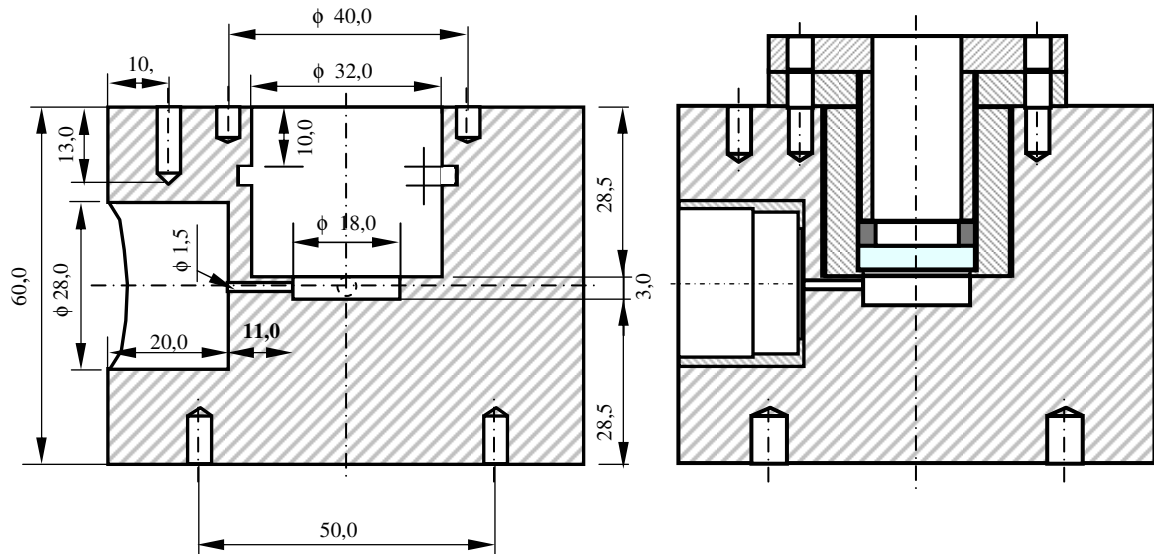


Figure 4.3. The photoacoustic cell used in experiments

Also in order to construct the criteria mentioned above, the pressure oscillation amplitudes in our cell gas were detected by a Brüel & Kjaer (B&K) Type 4144 1" pressure-field microphone. Type 4144 is a microphone where the damping of the diaphragm is such that the pressure frequency response is flat over a wide frequency range. Hence no correction is needed to the pressure below 8 kHz [19]. In order to amplify the signal detected by microphone, a preamplifier is needed. For this reason, in the experiments for 1" Type 4144 microphone a B&K Type 2673 preamplifier was used. This

preamplifier was connected to B&K Type 2610 Measuring Amplifier with AO0419 type cable, in order to increase the level of very low signal.

4.3. Data Acquisition

The tasks of acquiring, storing, and displaying the data can be performed in many ways. However, certain basic procedures should be followed. For example, the signal from the microphone preamplifier should be processed by an amplifier tuned to the chopping frequency, in order to maximize signal to noise ratio (SNR). If phase as well as signal amplitude is desired, or if very weak signals are to be measured, then a phase-sensitive lock-in amplifier should be used. Lock-in amplifiers are used to measure amplitude and phase of signals buried in noise. They achieve this by acting as a narrow band pass filter which removes much of the unwanted noise while allowing through the signal which is to be measured [20].

For a single-beam spectrometer, provisions must generally be made to remove, from the photoacoustic spectrum, any spectral structure due to the lamp, monochromator, and optics of the system. This normalization of the PAS signal to constant input light intensity can be achieved in two ways with essentially equivalent results. In Method 1 (shown in Figure 4.4) a detector is used to sample a portion of the modulated light beam incident on the cell, followed by a second lock-in amplifier. The ratio $S_{\text{PAS}}/S_{\text{Detector}}$ is obtained using the analog ratio meter option in the second lock-in amplifier. In Method 2 (shown in Figure 4.1) the PAS spectrum from a carbon black sample is stored in the memory of a multichannel analyzer as a reference signal proportional to the incident light. The PAS spectrum of the sample under study is then measured in a separate experiment and also stored. The ratio of these signals is evaluated numerically. The sample substitution reproducibility and temporal stability of the PAS spectrometer are such that the ratio is independent of $I_0(\lambda)$ to within the accuracy of the experiment [21].

That is to say, spectral features due to the light source and optics are removed from the sample spectrum by a ratio of the sample signal to the signal from a black-body absorber like carbon-black [8]. For carbon black, $(k_s) \approx 10^3 \text{ cm}^{-1}$ and $\beta \approx 10^6 \text{ cm}^{-1}$ [6]. And this black is a spectrally flat optical absorber for photoacoustic spectroscopy [16].

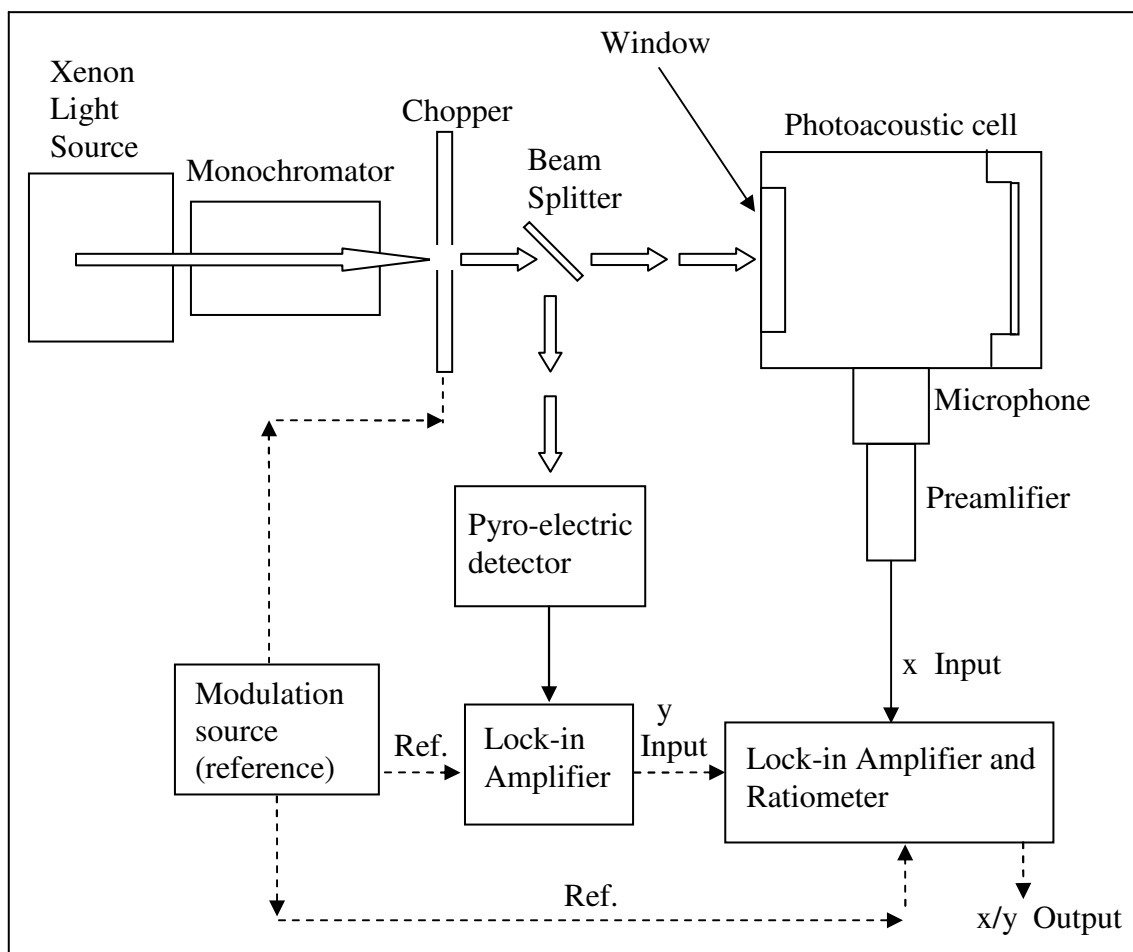


Figure 4.4. The photoacoustic spectrometer block diagram [21]

In a double-beam spectrometer, normalization can be performed in analog real-time fashion, by dividing the analog output from the tuned amplifier processing the sample signal by the output derived from a reference signal. This reference output may be from a power meter or from a second photo-acoustic cell containing a black absorber.

The digital data acquisition system furthermore permits to perform various data analyses and plotting routines, and to do multiscan experiments when studied with very weak signals.

For our system, shown in Figure 4.1, an SRS850 lock-in amplifier was used in order to filter out the amplified signal by locking at the chopper frequency; and in our set up, the spectrometer was controlled through a Visual-Basic program, while the collected signal was averaged out and recorded in a personal computer.

5. EXPERIMENTS OF PHOTOACOUSTIC SPECTROSCOPY

5.1. General Outline

At TUBITAK UME Acoustical Group Laboratory, the PAS studies begun at the end of 2004. Approximately two years later, for fundamental PAS experiments, the experimental system was set up as shown in Figure 4.1. In this section of the thesis, the initial experimental studies on the PAS system are described and results are discussed.

In the first study, in order to minimize environmental noise in acoustical signal, the SNR of the system was investigated by using a chopped monochromatic light source.

In the second study, in order to detect whether the experimental results obey the Rosencwaig-Gersho theory, the changes on photoacoustic signal were measured for an optically opaque material (lampblack) by changing the chopping frequency of incident light. At the end, the results were compared with the theory.

Thirdly, by using lampblack as sample, the reference spectrum of the system (lamp, monochromator and optical system) was determined and interpreted.

In a later study, the absorption spectrum of blood was obtained by using our PAS system, and the results were compared with the spectrum of blood that was obtained with a visible optical absorption spectrometer.

In the last study, in order to attribute a standard sensitivity to our PAS cell and to allow quantitative measurements at different frequencies, we calibrated the PAS cell by measuring its acoustic response under the optical heating and electrical heating of the sample.

5.2. General Description of the Apparatus

The photoacoustic spectrometer used in experiments is composed of three main parts: a chopped variable wavelength light source, an experimental chamber (cell) and the data acquisition system as shown in Figure 4.1. In the system an Osram XBO 450 W Xenon lamp was used as light source and its beam was focused on the entrance slit of a Jobin Yvon, Triax 550 model monochromator. The dispersed radiation from the exit slit was chopped by a Stanford Research Systems SR 540 model variable frequency chopper. The chopper causes approximately a 50 per cent duty cycle square wave illumination of the sample by monochromatic light which was focused in to the sample cell with a Melles-Griot concave lens. The pressure oscillation amplitudes in the cell gas were detected by a Brüel & Kjaer (B&K) Type 4144 pressure-field microphone followed by a B&K Type 2673 preamplifier with UA0786 model adaptor. After that, very low signal levels were stepped up by a B&K Type 2610 Measuring Amplifier. The amplified signal then was filtered out in a Stanford Research System SR850 lock-in amplifier and locked to the frequency of the chopper. In the photoacoustic spectrometer set up, all system was controlled through a Visual-Basic program and collected signal was averaged out and recorded in a personal computer. In some measurements a Melles-Griot 633 nm He-Ne gas laser in the 5 mW power range was substituted for the xenon lamp and monochromator.

5.3. Signal to Noise Ratio

The photoacoustic effect can be used to obtain optical absorption data on all types of materials. In addition, by changing the chopping or modulation frequency, a depth-profile analysis of the optical properties of a material can be obtained. At high chopping frequencies, information about the near regions of the sample surface was obtained, while at low chopping frequencies the data come from deeper within the sample. That is to say, the thermal diffusion lengths in the cell and sample depend on the modulation frequency and hence the cell response is frequency dependent. This is a feature unique to the photoacoustic technique.

In a PAS system, high sensitivity and high performance is needed for varying and fixed chopping frequency. The most serious limitation to high sensitivity of PAS system is

the background photoacoustic signal from absorption of the optical beam in the cell windows, and from absorption of scattered radiation by the cell walls. Additional background acoustic noise can arise from ambient acoustic and building vibrations, and electromechanical light chopping systems. Electronic noise of the amplifier connected to the microphone also has contribution to decrease the performance of the photoacoustic system. In order to enhance the reliability of the experimental results, the noise contributing effects of the cell and the ambient conditions must be minimized. One way of doing this is to determine the SNR of the system as a function of chopping frequency. By using a lampblack (carbon black) as the sample, the SNR of our system was determined. As stated in Section 4, carbon black is a strong absorber in the visible region of the spectrum and couples well thermally to the cell gas, thus providing an indication of the maximum signal levels that can be expected from the cell. The cell response was measured with 2 mm monochromator slit width at 425 nm wavelength, with a 300 msec amplifier time constant setting between 30 and 100 Hz chopper frequencies.

For each frequency value the SNR of the PAS system is shown in Figure 5.1. The SNR has its highest value at 85 Hz. For this reason, in order to minimize the effect of noise on experimental results, 85 Hz will be the working frequency of our system whenever a variable wavelength but a fixed modulation frequency is used in future experiments.

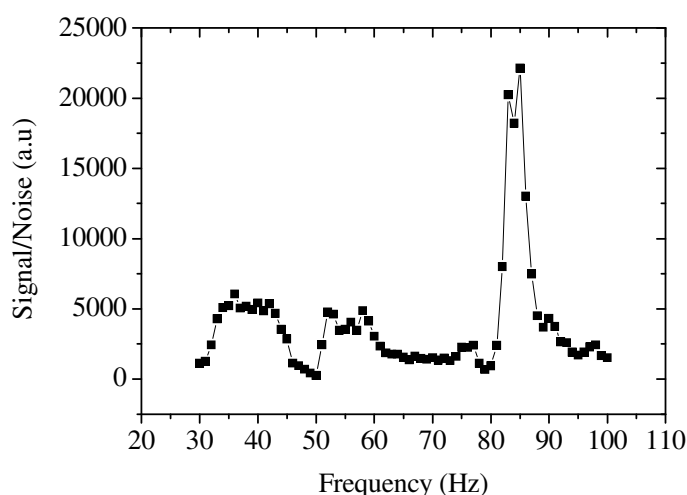


Figure 5.1. Signal to noise ratio of the photoacoustic system

5.4. The RG Theory

We also did experiments to see that if our system obeys the RG theory. In these experiments, the changes on photoacoustic signals were determined for a fixed wavelength and variable chopping frequencies by using a 5 mW power He-Ne laser as light source and a homogeneous thin layer of lampblack (carbon black) as sample.

As stated in Section 3, according to RG theory, for an optically opaque material ($l_{\beta} < l_s$) like carbon black, the PAS signal varies as ω^{-1} when $\mu_s > l_{\beta}$. That is to say, if our system is working according to RG theory, a log-log plot of the photoacoustic signal versus chopping frequency for lampblack must show a frequency dependence that varies close to ω^{-1} . In the Figure 5.2 the experimental results are shown. The slope of the line is found to be -0.92. This obtained value is near the theoretical value of $\kappa = -1$. So we can say that our system obeys the RG theory for optically opaque samples.

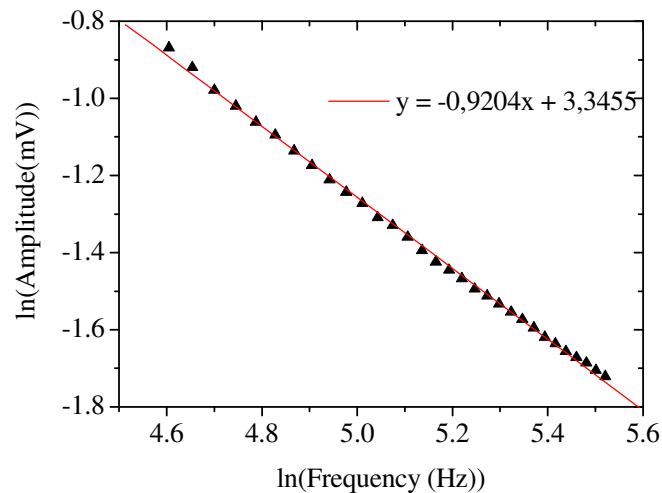


Figure 5.2. A log-log plot of the photoacoustic signal versus chopping frequency for lampblack

5.5. The Photoacoustic Spectrum of Carbon Black

One of the most obvious and important prediction of the Rosencwaig-Gersho theory is that the photoacoustic signal is always linearly proportional to the power of the incident photon beam, and this dependence holds for any sample or cell geometry. In Section 3, it

was shown that when the thermal diffusion length in the sample is greater than the optical absorption path length (Sections 3.2.1, and 3.2.2), the photoacoustic signal is independent of the optical absorption coefficient of the sample. In these cases, therefore, the only term in (3.13) or (3.14) that is dependent on the wavelength of the incident radiation is the intensity I_0 of the light source. Thus it is clear that the photoacoustic spectrum in the case of a photoacoustically opaque sample ($\mu > l_\beta$) is simply the power spectrum of the light source. It is also known as the reference spectrum of the system, since this spectrum is used to obtain the unknown spectrum of a sample with using one of the normalization processes stated in Section 4.3. So, in our experimental system, shown in Figure 4.1, by using a lampblack as sample, we tried to verify this theory and got the spectrum shown in Figure 5.3. In Figure 5.4 the real spectrum of Osram XBO 450 W xenon lamp, taken from the reference, is shown. There are minor differences between measured and real spectra. These differences come from the contributions from the monochromator and the optics in the experimental system. That is to say Figure 5.3 is not only the spectrum of Osram XBO 450 W xenon lamp; it is the reference spectrum of the total system consisting of xenon lamp, monochromator, and optics.

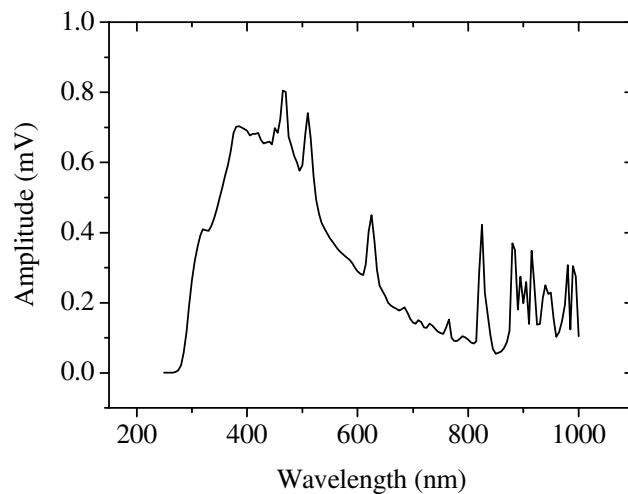


Figure 5.3. The reference spectrum of system

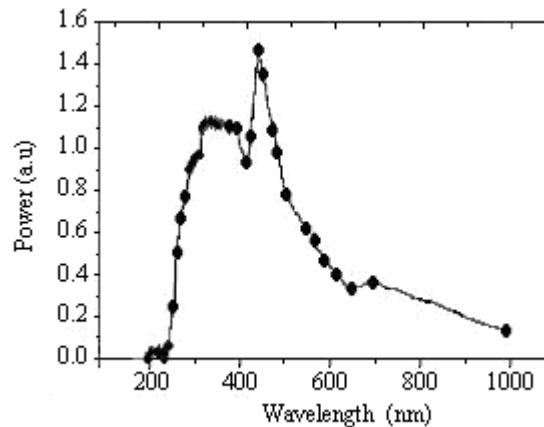


Figure 5.4. The spectrum of Osram XBO 450 W xenon lamp [11]

5.6. The Absorption Spectrum of Blood

A main advantage of the PAS applied to solids is the fact that no elaborate sample preparation is required and unpolished sample surfaces cause no problems. Since the photoacoustic signal is proportional to the absorbed energy, PAS permits measurements of spectra of even strongly scattering samples. The measurement of minimum absorption coefficients of 10^{-6} cm^{-1} corresponding to absorbed laser pulse energies of only 1nJ is possible [22].

The inherent high light scattering and the often strongly varying depth structure render biological and medical samples rather difficult for investigation with spectroscopic tools. However, photoacoustic technique can be successfully applied to media such as skin tissue and blood [22]. The ability of the PAS to detect specific compounds present in a highly diffusive medium is another advantage in spectroscopic studies on blood. Requirement of very minor amount of blood for studies is another advantage over other conventional techniques. For these reasons, we studied blood also by using the PAS technique. On a 1 cm^2 glass it was put a drop of blood and then this sample was placed inside the cell. By using the data acquisition system, a spectrum was obtained between the wavelengths of 400 nm and 700 nm. The automation of measurements was based on the following algorithm:

- The computer tells the monochromator to turn the grating turret until obtaining 400

nm at the exit slit.

- In this wavelength volume, the computer starts recording and averaging the voltage values from the lock-in amplifier. The aim of the averaging is to minimize the effect of sudden voltage fluctuations induced by possible external noise sources.
- Then the turret is turned with the wavelength interval specified at the beginning as 5 nm.
- The same procedure continues from step two until at the exit slit the wavelength value is 700 nm.

The spectrum was obtained at the end of this process is not the real spectrum of blood since it contains the spectrum of light source, monochromator and optics. So, the spectrum of lamp black was used to remove the spectral features due to the light source, monochromator and optics from the spectrum of blood. As a consequence, the real spectrum of blood was obtained as shown in Figure 5.5. This figure also shows another spectrum of blood which was obtained by using a Varian 5500 model visible region absorption spectrometer. As seen from the figure, these two spectra have similar behaviors. Both of them exhibit absorption bands at 415, 540, 580 nm which are caused by tetraporphyrin cycle bound to the blood's amino acid skeleton. It means that, the spectrum of the blood, which was obtained by photoacoustic technique, gives the correct absorption bands. One important difference between the optical spectrometer measurement and PAS measurement is the different wavelength sensitivity of the spectrometers. Sensitivity of the measurements depends on the photoacoustic cell structure. For this reason, we have to approve the quality of the cell by calibrating it.

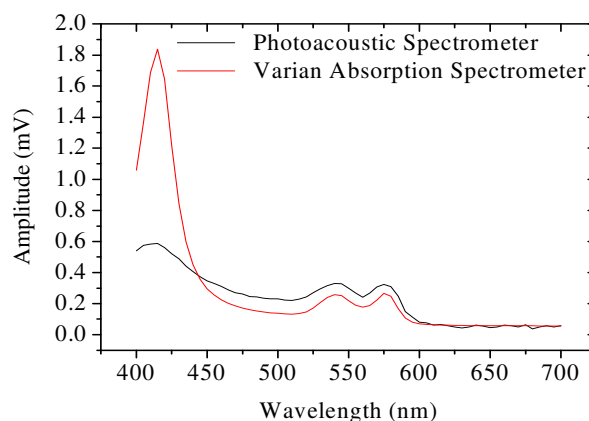


Figure 5.5. The absorption spectrum of blood

5.7. Calibration of the Photoacoustic Cell

In a PAS system, the photoacoustic signal is dependent on various parameters of cell design, gas type and pressure, backing material properties, microphone parameters, and so on. Since the basic objective of a PAS experiment is usually the determination of the sample properties, these cell-dependent effects are experimental impediments which must be removed. Fortunately in a fixed modulation frequency operation of a single cell, these complications do not interfere with the wavelength dependent measurements of the sample. However, for those experiments involving the variations in modulation frequency, it is necessary to calibrate the cell effects independent of the sample effects. That means, in order to specify a “standard” sensitivity for different PAS cells (independent of sample effects) and to allow quantitative measurements at different frequencies, calibration of these cell effects independent of the sample effect is important [7].

In order to calibrate the PAS cell directly in terms of absolute energy units, an electrically conductive metal black was used. Since the metal black sample serves as a spectrally flat optical absorber (similar in principle to carbon black), it is used by many workers as a reference material in photoacoustic spectroscopy studies [7]. It also serves as a uniform thermal source under resistance heating when connected to an external voltage or current source. In the experiment, to minimize the effects of thermal diffusion and heat capacity, which can alter the rate of heat transfer from the surface to the gas, the metal black was formed as a thin film [23].

At the beginning of the experiments our purpose was to use platinum thin film as a metal black, because of good thermal conductivity and excellent electrical conductivity of platinum. For this reason, in a vacuum deposition chamber, a chromium layer of thickness 100 \AA was deposited on to a glass substrate, than on this chromium layer, a thin platinum layer of thickness 100 \AA was deposited. After these deposition processes in order to convert the platinum thin film to a platinum “black”, we polarized platinum thin film cathodically for two minutes in a two per cent solution of chloroplatinic acid at 100 mA/cm^2 [24]. Electrochemical blackening of thin films is known to produce surface areas as high as 10^5 times greater than the geometric area. But, our effort to obtain a good platinum black failed. When this film was plunged in to the chloroplatinic acid, the surface

morphology of platinum was changed. There were cracks on the surface and the colour was not black. For this reason we decided to try another method to obtain a metal black.

In this method, gold was used instead of platinum since it is cheaper than platinum and it is easier to evaporate. Firstly, gold was placed on a tungsten wire, and the evaporation chamber was evacuated to a pressure of $1\mu\text{bar}$. The tungsten wire was outgassed and a small amount of gold evaporated to make sure that the absorbed gases and impurities in gold are removed. After that, argon gas was admitted to the chamber until the pressure was 0.65 mbar, the current through the tungsten wire was raised and the shutter opened so that the gold started to deposit on to a 1 cm^2 glass substrate. The distance between the evaporant source and the substrate and the residual gas pressure during the evaporation were kept constant, they were 7 cm and 0.65 mbar respectively [25]. At the end of this process we got a gold black thin film with a resistance of approximately 30Ω . Figure 5.6 shows the medium resolution Atomic Force Microscopy (AFM) picture of the gold black surface. As seen from the figure, the black color of gold comes from the geometrical roughness of its surface.

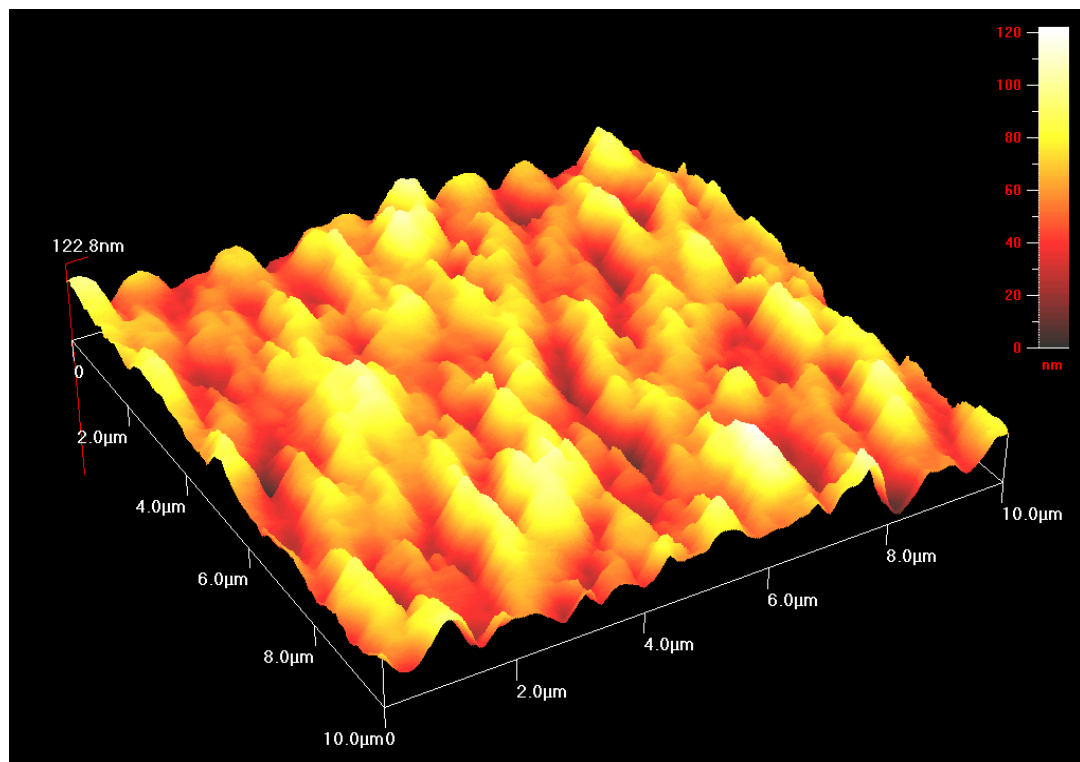


Figure 5.6. The medium resolution AFM picture of the gold black surface

Then this gold black was placed inside the photoacoustic cell shown in Figure 5.7. This instrumental configuration used to measure sound pressure levels produced in an air-filled cell by both optical and electrical heating of the gold black. In both cases, measurements were made in a frequency range between 30 Hz and 250 Hz.

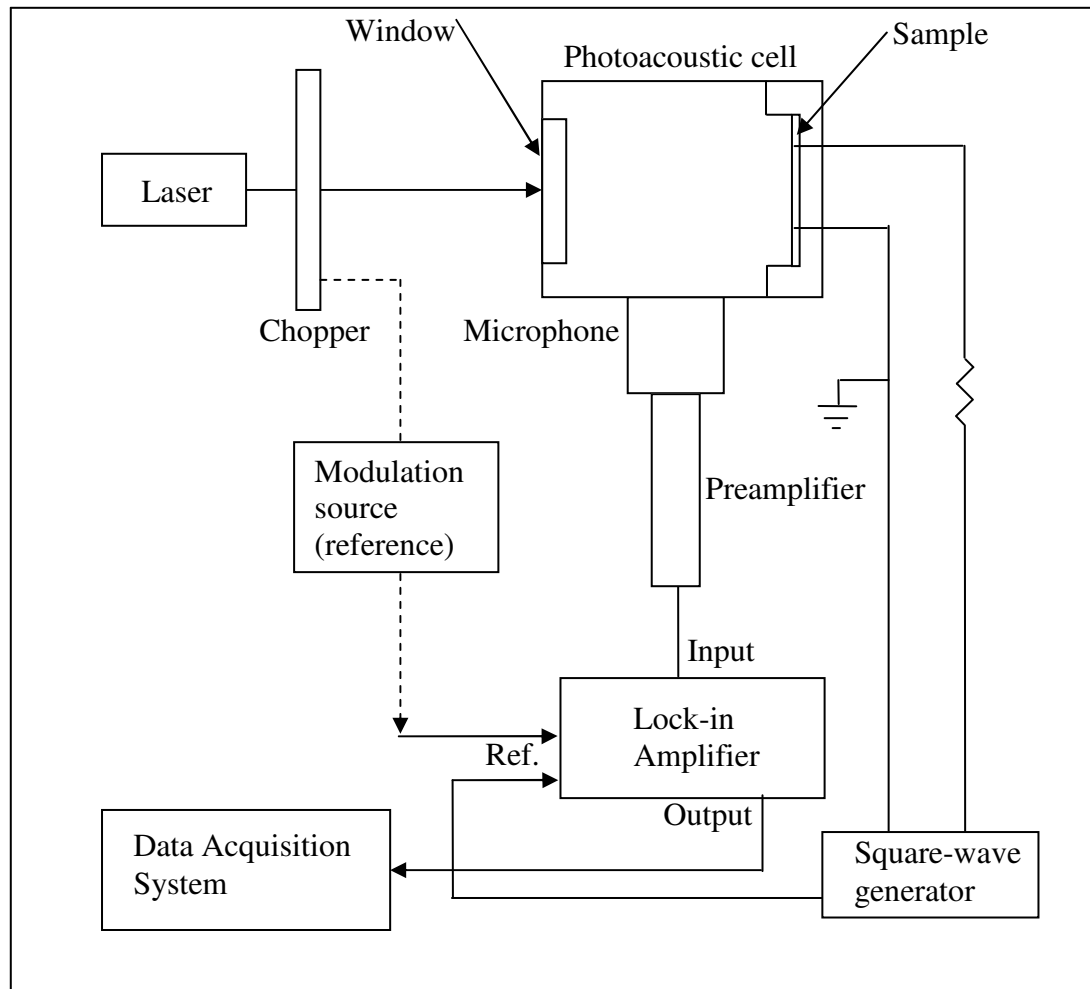


Figure 5.7. The photoacoustic system for gold black thin film measurements

In the initial experiments, the gold black in the photoacoustic cell was illuminated by a Melles Griot He-Ne laser at wavelength of 633 nm and 5 mW power at 30 Hz chopper frequency. Energy in the modulated incident light beam is partially absorbed by the gold black, and internally converted to heat, and subsequently this heat is transferred to the gas in thermal contact with the sample. This cyclical heating and cooling of the gas around the sample produces a periodic pressure change which is detected by the B&K Type 4144 microphone. This detected signal was recorded by the data acquisition system.

Measurements were done from the frequency of 30 Hz up to 250 Hz with 5 Hz steps. In Figure 5.8, the acoustic intensity versus modulation frequency under the optical heating effect is shown.

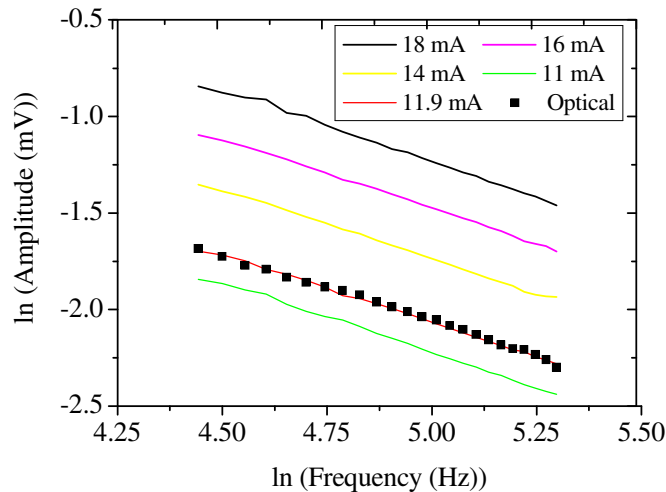


Figure 5.8. The acoustic intensity versus modulation frequency for both optical and electrical heating of gold black

Some measurement processes were repeated for electrical heating of the gold black. In this case, we used a square wave generator which produces a current between 0 and 20 mA with frequency between 0 and 250 Hz. In order to get electrical heating, first of all, the square wave generator's current value was fixed and for this fixed heating current value, the frequency was changed from 30 Hz to 250 Hz with 5 Hz steps. Then the produced acoustic signal was measured at each frequency value. As a result, for that value of heating current, we got a graphic showing the acoustic intensity versus modulation frequency. We measured the photoacoustical signal for the heating current range of 0 to 20 mA. A portion of these experimental results is shown in Figure 5.8. For this figure the optical data graphic which was obtained from optical heating of gold black with 5 mW laser, lies on the line $P_0=4.25$ mW obtained from the electrically heated results. That is to say all of the laser power is not converted to heat. The photoacoustic cell reduces the power of incident light approximately 0.75 mW, because of the optics and backreflections. By using this result, it is possible to determine the power of any lamp source. So a photoacoustic system can be used as a light power meter. On the other hand according to this graphics, the measured acoustic response is the same for both optical and electrical heating and the frequency

dependent cell effects are identical in both cases. The optical response can then be measured in terms of the electrical input power. Such a device is known as photothermophone (PTP). By using PTP technique, it has been possible to separate the optical and thermal properties and to concentrate on the thermal effects alone.

Finally, the calibration of the PAS cell responsivity described above applies only to the cell related effects. It does not provide a means of quantifying sample related effects which also affect the amplitude and frequency response of the PAS signals and depend upon the thermal diffusion lengths and optical absorption lengths in the sample.

6. CONCLUSIONS

In this thesis, the photoacoustic spectroscopy (PAS) experimental system was set up at the National Metrology Institute (UME) of the Scientific and Technological Research Council of Turkey (TUBITAK) in order to make spectroscopic research on solid samples. The confirmation of whether the system is working according to the Rosencwaig – Gersho (RG) theory was explored. The results obtained with this system were also compared with visible light optical absorption spectroscopy.

High sensitivity of the PAS system is very important for doing experiments with both variable and fixed chopping frequency. However, background acoustic noise in the system, limits the performance of the PAS research. In order to enhance the reliability of experimental results, the noise contribution coming from cell structure and ambient conditions has to be minimized. In this study by using a lampblack as sample, we determined the signal to noise ratio (SNR) of our photoacoustic system for different chopping frequencies, and we found that SNR was maximum at 85 Hz. So for the fixed modulation frequency case, to minimize the effect of noise on the experimental result, 85 Hz must be the frequency of our system.

In addition to that, to see whether our PAS system is working well according to the RG theory, which is the fundamental theory of PAS, the changes on photoacoustic signals were determined for a fixed wavelength and variable chopping frequency. In result, we got a log-log plot of the photoacoustic signal versus chopping frequency where we found the slope of the line to be -0.92 as apposed to -1.0 for the RG theory. Consequently, we can say that the obtained value is compatible with the theoretical value and the system is working well in accordance with the RG theory.

In addition to these studies, in order to confirm that it is possible to obtain a spectrum of highly diffusive sample using our photoacoustic experimental system, we investigated blood spectra. For normalization process, the total spectrum of light source, monochromator and optics was used as the reference spectrum of the system, and as a result we succeeded to obtain the absorption spectrum of a healthy human blood sample.

This spectrum was very close to the blood spectrum which was obtained from a visible region absorption spectrometer. Our system clearly distinguished the absorption bands at 415, 540, 580 nm. From these measurements, we can say that our PAS system can be used successfully for spectroscopic investigations.

Since the basic objective of a PAS experiment is usually the determination of the sample properties, the cell dependent effects are experimental impediments which must be removed. In order to specify a standard sensitivity to our PAS cell or to allow quantitative measurements at different frequencies we calibrated our photoacoustic cell by heating a gold black thin film, which is a spectrally flat optical absorber and a uniform source for resistance heating when connected to an external voltage or current source, both optically and electrically. We measured almost the same acoustic response for the electrical and optical heating. As a result, we can say that our photoacoustic system can be used as a calorimeter which is also called as photothermophone (PTP). After these measurements, it became possible to separate the optical and thermal properties and to concentrate on the thermal effect alone.

In conclusion, as a result of two years study, the PAS system was set up successfully according to its theory. It was used for both spectroscopic and calorimetric studies. In future studies, we aim to use PAS on a microscopic scale to perform photoacoustic microscopy (PAM) in order to investigate the cracks on surfaces and to measure the thickness of thin films and thin film layers, and to perform nondestructive testing (NDT) in order to obtain depth profile analysis of the samples.

REFERENCES

1. Bosquet, P., *Spectroscopy and Its Instrumentation*, Hilger, London, 1971.
2. Rosencwaig, A., *In Advances in Electronics and Electron Physics*, Academic Press, New York, 1978.
3. Rosencwaig, A. and A. Gersho, “Theory of the Photoacoustic Effect with Solids”, *Journal of Applied Physics*, Vol. 47, No. 1, pp. 64–69, January 1976.
4. Rosencwaig, A., *Photoacoustics and Photoacoustic Spectroscopy*, John Wiley, Canada, 1980.
5. Bell, A. G., “Production of Sound by Radiant Energy”, *The Manufacturer and Builder*, Vol. 13, pp. 156–158, July 1881.
6. Haisch, C. and R. Niessner, *Light and Sound - Photoacoustic Spectroscopy*, http://www.spectroscopyeurope.com/PA514_5.pdf, 2002.
7. Murphy, J. C. and L. C. Aamodt, “The Photothermophone, Device for Absolute Calibration of Photoacoustic Spectrometer”, *Applied Physics Letters*, Vol. 31, No. 11, pp. 728–730, December 1977.
8. McClelland, J. F. and R. N. Kniseley, “Photoacoustic Spectroscopy with Condensed Samples”, *Applied Optics*, Vol. 15, No. 11, pp. 2658–2663, November 1976.
9. Rosencwaig, A. and A. Gersho, “Photoacoustic Effect with Solids: A Theoretical Treatment”, *Science*, Vol. 190, pp. 556–557, November 1975.
10. Rosencwaig, A., “Photoacoustic Spectroscopy of Solids”, *Review of Scientific Instruments*, Vol. 48, No. 9, pp 1133–1137, September 1977.

11. Thomson, L. A. and G. J. Hageage, “Evaluation of Excitation Light Sources for Incident Immunofluorescence Microscopy”, *Applied Microbiology*, Vol. 30, No. 4, pp. 616-624, October 1975.
12. Horiba Jobin Yvon S.A.S., Model: Triax 550-552 Catalog, Longjumeau, 2004.
13. Stanford Research Systems, Model: SR540 Catalog, California, 2005.
14. Melles Griot, The Practical Application of Light Catalogue, California, 1999.
15. Aamodt, L. C. and J. C. Murphy, “Size Considerations in the Design of Cells for Photoacoustic Spectroscopy”, *Journal of Applied Physics*, Vol. 48, No. 3, pp. 927–933, March 1977.
16. Aamodt, L. C. and J. C. Murphy, “Size Considerations in the Design of Cells for Photoacoustic Spectroscopy II. Pulsed Excitation Response ^{a)}”, *Journal of Applied Physics*, Vol. 49, No. 6, pp. 3036–3045, June 1978.
17. Kinsler, L. E. and A. R. Freg, *Fundamental of Acoustics*, John Wiley, New York, 1962.
18. International Electrotechnical Commission, IEC 61094-2: Measurement Microphones; Part 2: Primary Method for Pressure Calibration of Laboratory Standard Microphones by the Reciprocity Technique, Switzerland, 1992.
19. Brüel & Kjaer, Type 4144 Technical Catalogue, Denmark, 1989.
20. İnanç, İ., *Temperature and Laser Power Dependence of Photoluminescence in Nanocrystalline Silicon*, M. S. Thesis, Boğaziçi University, 2004.
21. Murphy, J. C. and L. C. Aamodt, “Photoacoustic Spectroscopy of Luminescent Solids: Ruby”, *Journal of Applied Physics*, Vol. 48, No. 8, pp. 3502–3509, August 1977.

22. Markus W. S., *Electronic Spectroscopy Vibrational, Rotational and Raman Spectroscopies*, Academic Press, Switzerland, 1999.
23. Murphy, J. C., L. C. Aamodt and G. P. Warmar, "Surface Area Effect in Photoacoustic Spectroscopy", *Topical Meeting on Photoacoustic Spectroscopy*, Iowa, 1-3 August 1979, pp. 78–83, Elsevier, Washington, 1979.
24. Gileadi, E., E. K. Eisner and J. Pincier, *Interfacial Electrochemistry*, Addison-Wesley, England, 1975.
25. Thomas, S. and E. B. Pattinson, "The Controlled Preparation of Low SEE Surfaces by Evaporation of Metal Films under High Residual Gas Pressures", *Journal of Applied Physics*, Vol. 7, pp. 1469–1474, February 1974.